Theoretical and Applied Climatology (2025) 156:656
https://doi.org/10.1007/s00704-025-05894-1

RESEARCH

Performance and added value of a high-resolution (2 km) rainfall product based on WRF-downscaled ERA5 for Ho Chi Minh City, Vietnam

Tung Nguyen-Duy[1] · Thanh Ngo-Duc[2] · Marc Choisy[1,3] · Iago Perez Fernandez[4] · Sarah Sparrow[4]

Received: 25 August 2025 / Accepted: 5 November 2025

Abstract
Although the fifth-generation ECMWF reanalysis (ERA5) reanalysis dataset at 0.25º resolution and its land-specific product (ERA5-Land) at 0.1º resolution are widely used, they still remain too coarse for fine-scale applications. In this study, we dynamically downscaled ERA5 using the Weather Research and Forecasting (WRF) model to produce 2-km resolution rainfall data for Ho Chi Minh City, Vietnam (hereafter WRF-HCM). The model outputs were subsequently bias-corrected using quantile mapping, with daily data from 29 meteorological stations used for calibration and validation, resulting in products referred to as WRFC-HCM. Results show that, on a monthly scale, ERA5 generally outperforms WRF-HCM, WRFC-HCM, and ERA5-Land. However, on a daily scale, WRFC-HCM significantly improves accuracy, particularly in representing dry events. Seasonal probability density function analysis indicates that ERA5 overestimates light rain events, a bias substantially reduced by WRFC-HCM. For moderate and heavy rainfall (>20 mm/day), ERA5 underestimates occurrences, while WRFC-HCM provides better representation. Lastly, in assessing extreme climate indices, ERA5 and ERA5-Land overestimate the number of wet days, leading to higher Consecutive Wet Days (CWD) values, while underestimating heavy rain events, resulting in lower values for maximum 1-day precipitation (Rx1day) and maximum consecutive 5-day precipitation (Rx5day). These biases lead to an overall underestimation of rainfall intensity. Compared to ERA5, WRFC-HCM shows improved performance by effectively reducing the number of wet days and increasing Rx1day, offering a more accurate characterization of rainfall extremes.

Keywords ERA5 · Precipitation · WRF · Ho Chi Minh city · Dynamical downscaling

1 Introduction

Precipitation data are crucial for research across various scientific disciplines, particularly in hydrology, meteorology, and climate science. Accurate precipitation measurements are essential for hydrological modelling, which relies on precise data to simulate rainfall-runoff processes and predict water availability in river basins (Fraga et al. 2019). Furthermore, understanding precipitation patterns is vital for assessing the impacts of climate change, as shifts in

✉ Tung Nguyen-Duy
tungnd@oucru.org

Thanh Ngo-Duc
ngo-duc.thanh@usth.edu.vn

Marc Choisy
mchoisy@oucru.org

Iago Perez Fernandez
iago.perezfernandez@eng.ox.ac.uk

Sarah Sparrow
sarah.sparrow@oerc.ox.ac.uk

[1] Oxford University Clinical Research Unit, Ho Chi Minh, Vietnam

[2] Department of Space and Applications, University of Science and Technology of Hanoi (USTH), Vietnam Academy of Science and Technology (VAST), Hanoi, Vietnam

[3] Centre for Tropical Medicine and Global Health, Nuffield Department of Medicine, University of Oxford, Oxford, United Kingdom

[4] Department of Engineering Science, University of Oxford, Oxford, UK

Published online: 17 November 2025

precipitation can lead to changes in flooding, droughts, and other extreme weather events that significantly affect human societies and natural environments (Tabari, 2020; Ukkola et al. 2020).

Precipitation data from rain gauges are generally considered as the most accurate rainfall sources, however, it comes with several limitations. The first issue is the sparse distribution of rain gauges, which often leads to inadequate spatial coverage, especially in the mountainous or remote area (Hong et al. 2006). Additionally, the rain gauge data availability might be discontinued over time. For example, data might be unavailable during times of war, or at stations located in remote areas that might be inaccessible to maintain the devices regularly. All of these can lead to gaps in rain gauge data throughout the study period, and thus, data availability might affect the results of long-term studies.

With the development of space technology, satellites can also provide precipitation data. Satellite data can offer high spatio-temporal resolution, which is crucial for tracking precipitation events in real-time, particularly in the context of hazardous weather systems (So and Shin 2018). Additionally, satellite precipitation data can improve the accuracy of hydrological predictions, particularly in regions with limited ground observation networks (Behrangi et al. 2011). However, satellite precipitation products are often influenced by various uncertainties, including instrumentation errors and algorithmic limitations in estimating rainfall across different temporal and spatial scales (Hong et al. 2006).

Global reanalysis datasets, such as the fifth generation European Centre for Medium-Range Weather Forecasts (ECMWF) reanalysis (hereinafter referred to as ERA5), are created to overcome the limitations of gauges and satellite data. It provides data over a long period of time and integrates vast amounts of observational data from various sources, including satellites and ground stations, into a coherent framework through advanced data assimilation techniques (Hersbach et al. 2020). Moreover, the continuous updates and extensive historical coverage of ERA5 (with the horizontal resolution of 31 km), as well as its high resolution dataset over land – ERA5-Land (9 km; Muñoz-Sabater et al. 2021) – facilitate monitoring and long-term climate analysis, thereby supporting informed decision-making in various sectors such as simulating offshore wind energy (Carvalho et al. 2014), modeling storm surge (Dullaart et al. 2020), predicting tropical cyclones (Winterbottom et al. 2012), and forecasting air quality (Feng et al. 2019). ERA5 products are more suitable than satellite data for climatic and hydrological applications on the Mongolian Plateau, particularly for analyzing interdecadal variability and trends (Xin et al. 2022). In agricultural research, ERA5 has been utilized to assess drought conditions and soil moisture trends. Almendra-Martín et al. (2022) highlighted the importance of ERA5 in analyzing agricultural drought trends on the Iberian Peninsula, emphasizing its role in providing reliable soil moisture data through satellite assimilation. In atmospheric science, using ERA5, Nguyen-Thanh et al. (2023) demonstrated the impacts of both ENSO and ENSO Modoki on rainfall variability over Southeast Asia. Ngo-Duc et al. (2024) used the ERA5 reanalysis dataset as the initial and boundary conditions for the RegCM4-NH experiments conducted over the CORDEX-SEA domain to identify and rank the best-performing parameterization schemes for simulating temperature and rainfall over Southeast Asia, which will aid in future downscaling of CMIP6 GCM outputs in this region.

While ERA5 is widely used, it still has some limitations. First, it may contain errors, due to the model itself, or due to its relatively coarse spatial resolution that cannot resolve all the processes, especially in areas with complex topography. In Spain, ERA5 and ERA5-Land tend to overestimate light and moderate rain (from 1 to 20 mm/day) while underestimating heavy rain (more than 20 mm/day) (Gomis-Cebolla et al. 2023). A wet bias of ERA5 is also observed in Africa (Steinkopf and Engelbrecht 2022). ERA5 underestimates the frequency of heavy rainfall events while overestimating the number of wet days (Gbode et al. 2023; Xin et al. 2022). Although having higher resolution, ERA5-Land still exhibits some errors due to local microclimatic conditions and bias correction is still required (Longo-Minnolo et al. 2022) and does not always outperform the lower resolution ERA5 (Gomis-Cebolla et al. 2023).

Additionally, given its relatively coarse horizontal resolution (approximately 25 km), ERA5 remains insufficient for certain fine-scale studies, highlighting the need for higher-resolution data. For this reason, downscaling has been implemented to create local, high-resolution data from coarser global or larger-scale datasets. Popular downscaling methods are statistical (Gutmann et al. 2012; Manor & Berkovic, 2015; Tran-Anh et al. 2023), dynamical (Zhang et al. 2018; El-Samra et al. 2018; Ngo-Duc et al. 2024) and hybrid (Tran Anh & Taniguchi, 2018). Statistical downscaling methods are typically computationally efficient and significantly faster than dynamical downscaling. However, they depend on the assumption of a stable statistical relationship over time and require extensive historical climate observation data for validation, which may not be available in all regions (Tran Anh & Taniguchi, 2018). Dynamical downscaling, on the other hand, is based on physical mechanisms and incorporates complex local processes, allowing to capture fine-scale features that are not resolved by coarser-resolution products (El-Samra et al. 2018). This approach is particularly effective at reducing errors in regions with complex terrain or in coastal areas, as the finer grid offers a more accurate representation of topography and coastlines.

(Heikkilä et al. 2011). However, dynamical downscaling can be computationally expensive and time-consuming, making it suitable only where sufficient resources are available.

Bias correction (BC) is an essential step for improving the reliability of climate model datasets. Trinh-Tuan et al. (2019) demonstrate that quantile mapping bias correction can significantly reduce precipitation bias in Vietnam, and improve the annual cycle in all climatic subregions. Additionally, they observe notable improvements in precipitation indices following bias correction. In hydrology, bias-corrected, dynamically downscaled precipitation data were shown to yield more accurate hydrological simulations compared to non-corrected data (Bastola & Misra,2014; Hagemann et al. 2011). In studies of extreme events, such as that by Evans et al. (2017), BC was shown to effectively reduce biases in extreme precipitation estimates.

Climate change is a serious threat to Ho Chi Minh City, with rising temperatures and sea levels. The city is also at risk of increased flooding, saltwater intrusion, and heatwaves, which could have severe implications for public health, agriculture, and urban infrastructure (Thanh Tu and Nitivattananon 2011). Therefore, having a high resolution of precipitation dataset is useful as an input for other models to provide more insight and accurate information to urban planning and development. At present, the highest-resolution rainfall datasets available for Ho Chi Minh City include global reanalysis products such as ERA5-Land (~10 km) and satellite-based datasets such as CHIRPS (~5 km). To our knowledge, our study represents the first effort to generate and evaluate a high-resolution (2-km) rainfall product for Ho Chi Minh City, Vietnam, obtained by dynamically downscaling ERA5 using the WRF model. We assess the performance and added value of the high-resolution rainfall dataset and its BC products over the study areas.

The rest of the paper is structured as follows: In Sect. 2, we present the methods and data used in this study. The comparison between the model and observational data is provided in Sect. 3, followed by the conclusions in Sect. 4.

2 Methodology

2.1 Study area

Ho Chi Minh city (HCMC) is the most populated city in Vietnam, with 9.4 million people (GSO 2023). It is located in the southeastern region of Vietnam, covering an area of approximately 2,061 km^2 (Fig. 1). The topography of Ho Chi Minh City is predominantly flat, with approximately 40–50% of its area lying below 1 m above sea level and an additional 15–20% between 1 and 2 meters above sea level (Vu et al. 2018). The city's geographical position plays a crucial role in its climate and hydrology, as it is influenced by both the tropical monsoon climate and the extensive river systems of the Mekong Delta.

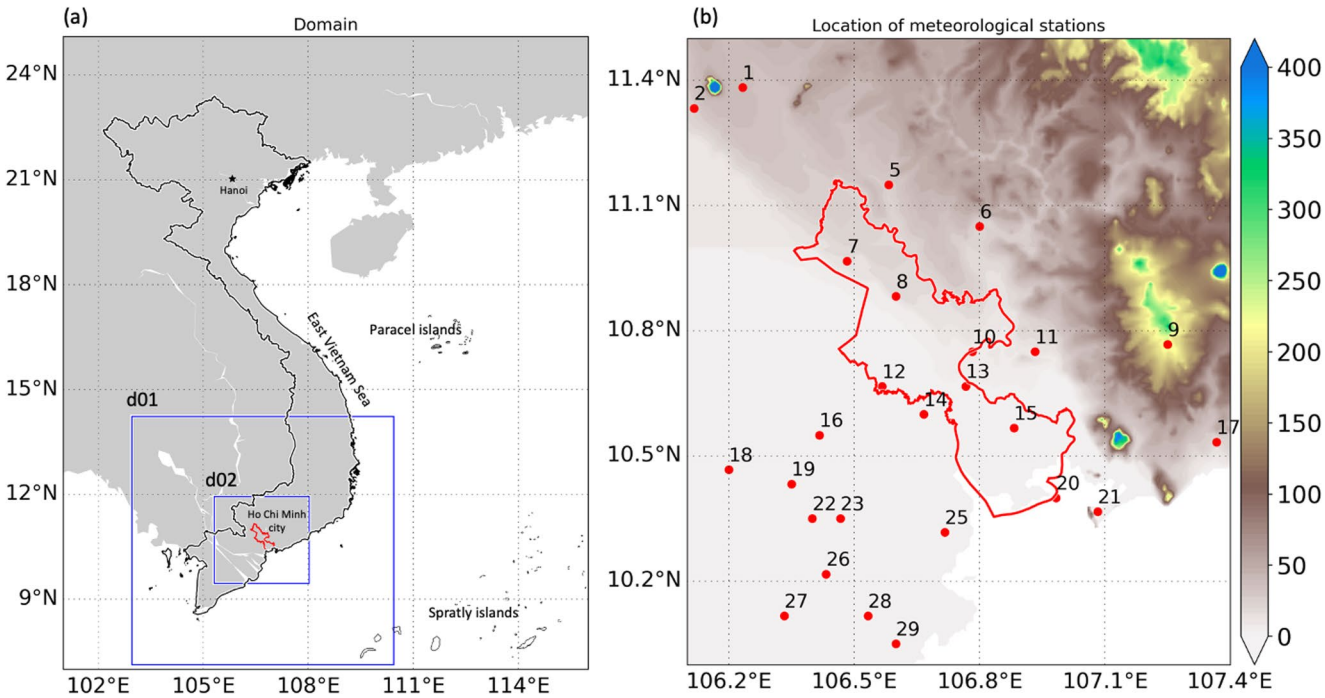

Fig. 1 (**a**) Location of Ho Chi Minh city (red polygon). d01 and d02 are the borders of the two WRF domains. (**b**) Elevation map of study area (Units in m). Numbers show the locations of the meteorological stations used for model validations

HCMC experiences a tropical monsoon climate, with two distinct seasons: the wet season, from May to November, and the dry season, from December to April. From 1997 to 2016, HCMC received an average rainfall of around 1600 mm/year, with more than 90% of precipitation occurring during the wet season from May to November. The average daily mean temperature in HCMC is around 27.3 °C, with lowest value in January (25.9 °C) and highest value in April (28.8 °C), which show minimal seasonal variation.

2.2 Model configurations

In this study, we use the WRF model, version 4.4 (Skamarock WC et al., 2019). It is a non-hydrostatic, primitive-equation model. WRF is designed to simulate atmospheric processes at high spatial and temporal resolutions, which is essential for capturing the complexities of weather systems. The model operates on a grid system that allows for dynamic downscaling, enabling researchers to focus on specific regions of interest while maintaining the influence of larger-scale atmospheric conditions (Srivastava et al. 2015). At the large scale, the WRF model is extensively used in various fields, from precipitation forecasts (Minh et al. 2018; Trinh et al. 2021) to regional climate downscaling (Tran Anh & Taniguchi, 2018; Chotamonsak et al. 2011), as well as modeling tropical cyclone (Tien et al. 2013). At the smaller scale, it is also used for urban climate studies (Doan et al. 2019). For instance, Kusaka and Hayami (2006) demonstrated the model's capability in simulating local weather events, highlighting its effectiveness in reproducing urban climatic effects. Miao et al. (2009) utilized WRF to investigate urban heat islands in Beijing, showcasing its ability to capture boundary layer structures influenced by urbanization. Moreover, WRF has been instrumental in evaluating and improving air quality models. Studies have shown that integrating WRF with air quality models enhances the understanding of pollutant dispersion and the impact of meteorological conditions on air quality (Kumar et al. 2017).

In this study, the grid of WRF is set up with 2 nested domains, named d01 and d02 (following the standard WRF naming convention), with horizontal resolution of 6 km and 2 km, respectively (Fig. 1a), using one-way nesting. Both grids are centered at HCMC center. The number of grid points for the d01 and d02 are 122×118 and 133×124, respectively. Both domains have 50 vertical layers, from surface to 50 hPa. The results from domain d02 (the innermost domain) are used for all the analysis.

The initial and lateral boundary conditions are taken from European Center for Medium-Range Weather Forecasts (ECMWF) ERA5. Lateral forcing was updated every 6 h at 0.25° horizontal resolution and 38 pressure levels. The physical parameterizations used include: (1) the SBU-YLin cloud microphysics scheme (Lin and Colle 2011); (2) the Kain-Fritsch convective scheme (Kain 2004) — applied for domain 1 but turned off for the domain 2; (3) the Dudhia shortwave radiation scheme (Dudhia 1989) (4) the Rapid Radiative Transfer Model (RRTM, Mlawer et al. 1997) used for longwave radiation; and (5) the Yonsei University planetary Boundary Layer scheme (Hong et al. 2010). This configuration was selected based on a sensitivity test that evaluated the model accuracy in reproducing daily precipitation.

To reduce overall delivery time, the entire simulation period can be divided into subperiods, each including a spin-up time (e.g. Jerez et al. 2018). The choice of spin-up duration varies between studies and often depends on the modeling objectives and the total length of the simulation. For instance, Cha and Wang (2013) used a 6-hour spin-up for a 3-day run, Jerez et al. (2018) applied a 4-month spin-up for a 5-year simulation, and Zhuo et al. (2019) used a 1-year spin-up for a 10-year run. In this study, the model was run in 17 subperiods covering the years 2000 to 2016, with each subperiod lasting 13 months, with the first month of each subperiod was allocated as the spin-up period. For example, for the year 2000, the model is run from 1/12/1999 to 31/12/2000.

2.3 Quantile mapping bias correction (QMBC)

Raw WRF results may exhibit substantial discrepancies compared to the observation (Tamaki et al. 2018). Therefore, in this study, we apply bias correction to the raw WRF results using the quantile mapping method. Quantile mapping is a widely utilized statistical technique for BC in climate modeling, particularly for precipitation and temperature data. This method operates by aligning the cumulative distribution functions (CDFs) of modeled data with those of observed data, effectively transforming the model outputs to better reflect the statistical properties of the observations. The process involves creating quantiles from the model data and mapping them to the corresponding quantiles of the observed data, which helps in correcting systematic biases inherent in climate models (Seenu and Jayakumar 2020; Lira-Loarca et al. 2023). The corrected value x_{cor} is:

$$x_{cor} = F_{obs}^{-1}\left(F_m(x_{simu})\right) \quad (1)$$

with F_{obs}^{-1} be the inverse empirical CDF of observed historical data, F_m be the empirical CDF of model historical data, and x_{simu} be the raw model-simulated value.

Several studies have demonstrated that quantile mapping can effectively adjust both the mean and extremes of

precipitation distributions, making it particularly valuable for applications related to hydrology and climate impact assessments (Maurer and Pierce 2014; Themeßl et al. 2011; Tran-Anh et al. 2023). In quantile mapping, the choice of probability distribution can significantly influence its performance. In this study, we choose to use the empirical quantile mapping method, which does not assume a specific distribution, since it can produce competitive results compared to other parametric approaches for correcting precipitation (Gudmundsson et al. 2012; Enayati et al. 2021).

Besides, there are several methods to subsampling the timescale to build the CDF. Sangelantoni et al. (2019) build the CDF for each day of the year using a 91-day sliding time window centered on that day. Other studies have used monthly (Ines and Hansen 2006) or seasonal subsampling. Reiter et al. (2018) demonstrated that the optimal subsampling timescale for correction varied depending on the quantile mapping method used, with a monthly timescale being optimal for both parametric and non-parametric quantile mapping approaches. Following their suggestions, in this study, we first correct the monthly result using monthly-subsampling data. The daily result is then rebuilt using the ratio between the daily and monthly precipitation.

To validate the effectiveness of the method, we divide the precipitation dataset into 2 parts. The first part, covers from 2000 to 2009, is used as a training dataset. The second part, spans from 2010 to 2016, is used as a validation dataset. All the comparisons in the results section use the data in the validation dataset.

2.4 List of experiments and datasets

The experiments used for performance evaluation are presented in Table 1. In addition to the results from the WRF model, including WRF-HCM and WRFC-HCM, we also evaluate the performance of the reanalysis products, ERA5 and ERA5-Land. ERA5-Land is a higher-resolution (10-km) product originated from ERA5, which focused exclusively on land areas (Muñoz-Sabater et al. 2021).

The experiments listed in Table 1 are evaluated using the rainfall observational data from 29 stations around HCM city. The results from all experiments are bilinearly interpolated to the locations of the stations before evaluation. The name and locations of the stations are shown in Fig. 1b. In addition to the station data, we also evaluated the CHIRPS satellite-based rainfall dataset (~5 km resolution) as a potential alternative reference for validation. The comparison with station observations using monthly data from 2010 to 2016 showed that the root mean square error and temporal correlation coefficient of CHIRPS were comparable to those of ERA5 and ERA5-Land (Supplementary Figure S1). Therefore, CHIRPS was not included in the final validation, as it did not provide additional added value compared to the station-based dataset.

Table 1 List of experiments used for performance evaluation

No	Name	Description
1	ERA5	ERA5 dataset (resolution: 25 km)
2	ERA5-Land	ERA5-Land dataset (resolution: 10 km)
3	WRF-HCM	Model results created from WRF (resolution: 2 km)
4	WRFC-HCM	Model results created from WRF, bias corrected using quantile mapping (resolution: 2 km)

2.5 Metrics and indices used in the assessment

We assess the performance of the experiments on both monthly and daily scales. For performance evaluation on the monthly scale, we employ three metrics including mean absolute error (MAE), correlation (CC), and root mean square error (RMSE).

For daily precipitation, the metrics mentioned above may not be applicable because precipitation data are typically dominated by non-precipitation days (zeros), which can distort RMSE results. Additionally, both MAE and RMSE do not consider the ability of a model to capture precipitation occurrence (e.g., whether it rains or not). Therefore, to more appropriately evaluate daily precipitation, we employ categorical statistical approaches. The description of the categorical statistics is provided in Table 2.

From the Categorical Statistics table, daily precipitation is evaluated using the Probability of Detection (POD), False Alarm Ratio (FAR), and Accuracy (ACC), which are defined below.

Probability of Detection (POD): a metric that measures the ability of an experiment to correctly identify the occurrence of observed rain events.

$$POD = \frac{a}{a+c} \tag{1}$$

False alarm ratio (FAR): a metric that measures the frequency of false alarms, i.e. the proportion of simulated rain events that did not actually occur in reality, relative to the total number of simulated rain events.

$$FAR = \frac{b}{a+b} \tag{2}$$

Table 2 Categorical statistic table

	Observed rain (≥1 mm/day)	Observed no rain (<1 mm/day)
Simulated rain (≥1 mm/day)	a (hit)	b (false alarm)
Simulated no rain (<1 mm/day)	c (miss)	d (correct no rain)

Accuracy: a metric that represents the proportion of correctly simulated events relative to the total number of events.

$$ACC = \frac{a+d}{a+b+c+d} \quad (3)$$

We note that the best value for FAR is 0, while the best value for POD and ACC is 1.

In addition to the metrics above, probability distribution functions (PDFs) for different seasons are computed to evaluate the frequency of various rainfall intensities.

For extreme events, we use a subset of indices that characterize rainfall extremes, suggested by the CCl/CLIVAR/JCOMM Expert Team on Climate Change Detection and Indices (ETCCDI) (http://etccdi.pacificclimate.org). Details of the selected indices are shown in Table 3. In this study, all the indices are computed on an annual basis.

3 Results

3.1 Performance evaluation at monthly time scale

The comparison of monthly precipitation from various experiments against observed data over the year, averaged over 29 stations is shown in Fig. 2. The observed data show a clear seasonal variation, with the wet season lasting from May to November, characterized by higher rain amounts of more than 4 mm/day, and the dry season lasting from December to April, with rain amounts less than 2 mm/day. The peak in precipitation occurs in late summer - early autumn (September-October) at more than 8 mm/day, while the minimum is in January and February, with less than 0.5 mm/day.

Compared to the observation, in general, all the experiments capture the seasonal pattern with the maximum value in September and minimum value in February. However, they still show some biases. WRF-HCM underestimates the precipitation from April to July, while overestimates the precipitation from August to December. The peak in September is strongly overestimated, reaching nearly 12 mm/day. QMBC works moderately, with reduced biases observed in WRFC-HCM, especially in September and October.

On the other hand, ERA5 overestimates the precipitation over the whole year. The difference between ERA5 and observation is smaller in the dry season, at less than 1 mm/day, but increases to around 2 mm/day in the wet season. Notably, although the WRF-HCM model is driven by ERA5 data (which exhibit overestimations consistently throughout the year), the WRF-HCM model exhibits a different seasonal pattern, with some months showing overestimations and others underestimations of rainfall. Similar to ERA5, ERA5-Land consistently overestimates rainfall throughout the year, and even slightly more so than ERA5.

The MAE, RMSE and CC of the different datasets are shown in Fig. 3. WRF-HCM has the highest MAE, averaging 2.24 mm/day. The error is higher in the north and lower in the south of the city. After bias correction, the results improve, with lower errors in all stations, averaging 1.96 mm/day. ERA5 has the lowest error among all datasets (MAE = 1.90 mm/day). The error is low in most of the stations except for one station in the south of the domain. Although having higher resolution, ERA5-Land has a higher MAE than ERA5, averaging 1.98 mm/day. For RMSE, WRF-HCM still has the highest error at 3.32 mm/day. Bias correction reduces the error to 2.84 mm/day. ERA5 remains highly competitive, with an error of 2.55 mm/day, the lowest error among all datasets.

For CC, the highest average correlation belongs to ERA5-Land ($r = 0.85$). The original WRF-HCM model has an average CC of 0.73. Notably, the bias correction does not help much in increasing the correlation, with the CC after bias correction being 0.75.

To explore the possible dependence between simulated precipitation and topographic condition, Fig. 4 presents the MAE of monthly mean values for stations categorized by elevation ranges. Across all elevation groups, the errors

Table 3 The ETCCDI indices used in this study

ID	Name	Calculation	Unit
PRCPTOT	Total precipitation in wet days	A wet day is defined as a day with precipitation ≥ 1 mm $PRCPTOT = \sum_{i=1}^{I} R_i$ with R_i being the precipitation amount of the wet day i	mm
Rx1day	Maximum daily precipitation	Rx1dayi = max (R_i) with R_i being the precipitation amount of the wet day i	mm
Rx5day	Maximum 5 consecutive days precipitation	Rx5day = max (R_j) with R_j being the total precipitation amount for 5 consecutive wet days	mm
SDII	Simple precipitation intensity index	$SDII = \frac{\sum_{i=1}^{I} R_i}{I}$ with R_i being the precipitation amount of the wet day i I represents number of wet days	mm/day
CDD	Consecutive dry days	Maximum number of consecutive days with daily precipitation < 1 mm	days
CWD	Consecutive wet days	Maximum number of consecutive days with daily precipitation ≥ 1 mm	days

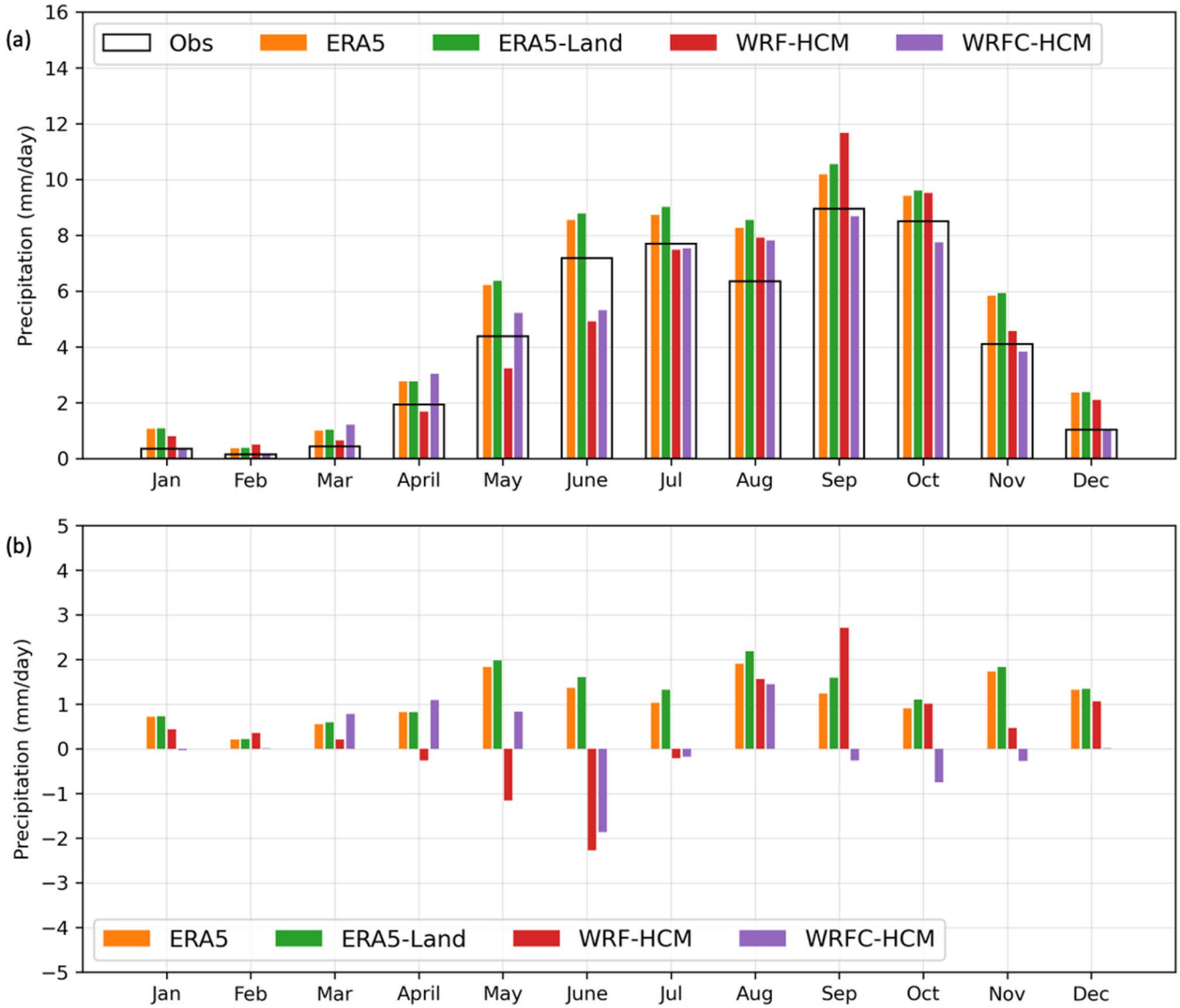

Fig. 2 **(a)** Monthly mean precipitation, averaged across 29 stations, based on validation data from 2010 to 2016 (white-filled bars) and model results (colored bars). **(b)** Differences between the validation data and the different simulations

are generally lowest in the DJF and MAM seasons, while higher errors are more prevalent during JJA and especially SON, which is explained by the lower precipitation in the winter and higher precipitation in the summer.

In DJF, the downscaling itself can improve the MAE, however, it does not seem to be related with the elevation. For elevations from 0 to 10 m and above 200 m, the error in WRF-HCM is lower than in ERA5, but for elevations from 10 to 50 m, the error in ERA5 is lower. In other seasons, the error in WRF-HCM is higher than in ERA5, except in MAM for stations located above 50 m. The bias correction works well, showing lower errors in WRFC-HCM across all elevation groups. However, the bias correction shows limited performance in MAM, when it tends to increase the error in all elevation groups, as shown in Fig. 2. In JJA, the error is lowest in ERA5 for all stations. In SON, for stations below 10 m, the error is lowest in WRFC-HCM, while for stations above 50 m, the error is lowest in ERA5-Land.

3.2 Performance evaluation at daily time scale

While performance at the monthly scale is useful for longer time scale studies, some analyses may require data at the daily scale. Therefore, the daily performance also needs to be assessed. Figure 5a represents the POD, which measures the ratio of correctly forecasted events to the total number of observed rain events. A higher value indicates better performance. Across all experiments, the POD varies from month to month. From May to November, most experiments show a higher POD, which is understandable since there are more

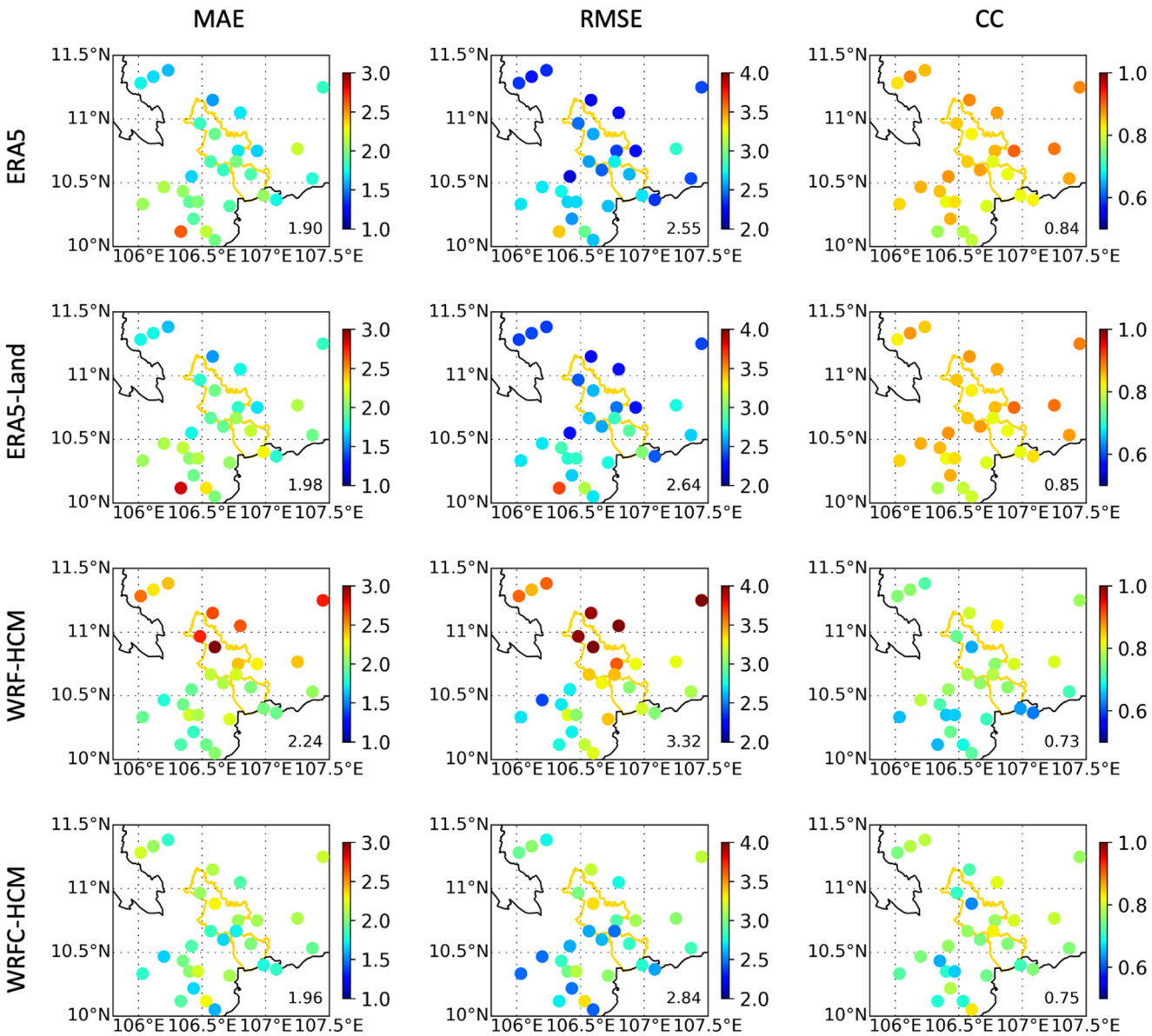

Fig. 3 MAE, RMSE, and CC (in row) of ERA5, and ERA5-Land, WRF-HCM, WRFC-HCM (in column) calculated using monthly data, from 2010–2016. In each subfigure, the numbers in the lower right corner indicate the mean values of all stations

rain events in this period. Overall, the POD of ERA5 is the highest over the whole year, ranging from 0.7 to nearly 1.0, while the WRF-based performance is lower, ranging from 0.3 to 0.7. During the rainy season only, WRF-HCM can capture about 70-75% of the rain events, while ERA5 and ERA5_LAND detect nearly all of them. However, since POD only measures the ability to capture rainfall events, an overestimation of the number of rainy days results in a high POD. In other words, POD can only assess the ability to predict rain events, ignoring the ability to predict dry events.

Figure 5b shows the False Alarm Ratio (FAR), which quantifies how often non-rain events are incorrectly forecasted as rain events. In contrast to POD, FAR is lower in the summer and higher in the winter. Notably, ERA5 and ERA5-Land tend to have higher FAR values throughout most of the year compared to the other experiments, confirming that the number of rainy days is overestimated. In detail, in winter, 80% of the rainy days in ERA5 are actually dry days in reality. This value is similar for WRF-HCM, but it decreases after bias correction. In rainy season, WRF-based results also provide an estimate of false rainfall of around 40%, which is better than ERA5 and ERA5-Land (47-50%).

The overall accuracy, representing the percentage of correctly simulated dry and rainfall days relative to the total number of days, is illustrated in Fig. 5c. Accuracy is highest

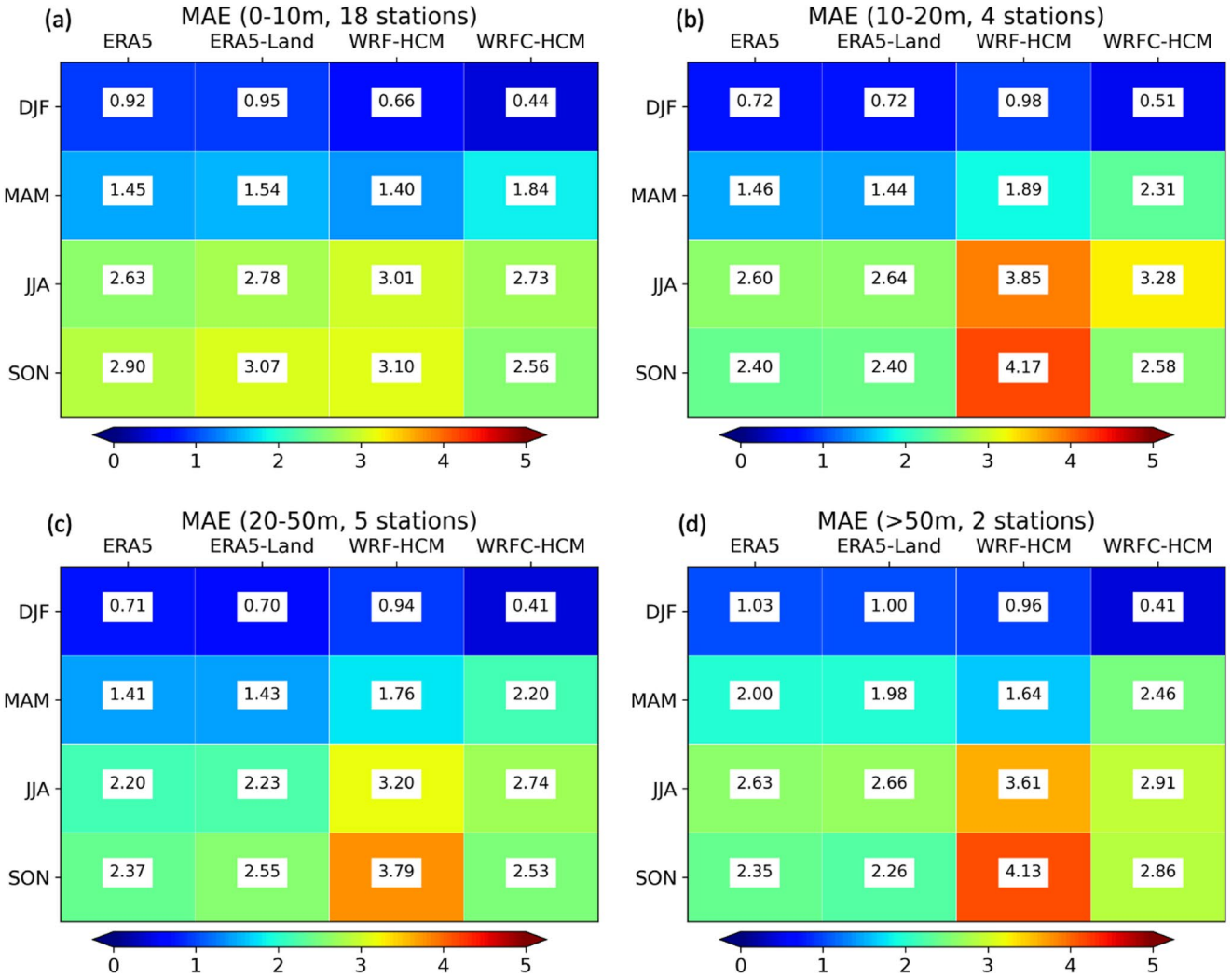

Fig. 4 MAE of monthly mean of precipitation in different seasons (December – February (DJF), March – May (MAM), June – August (JJA), September – November (SON)), grouping by elevation: (**a**) stations lower than 10 m, (**b**) stations from 10 to 20 m, (**c**) stations from 20 to 50 m, (**d**) stations higher than 50 m

at the beginning and end of the year, particularly in January and December, across all experiments, and lower in the rainy season. Among the models, the WRF-based experiments generally perform better. The bias correction improves the overall accuracy mostly in the dry season (from December to February) but shows no clear difference in the rainy season. Since they have lower POD values, the higher accuracies of the WRF-HCM and WRFC-HCM experiments indicates better performance in representing dry events compared to the reanalysis products. To further evaluate the added value of the dynamical downscaling process beyond bias correction alone, the same bias-correction and validation procedures were also applied to ERA5 and ERA5-Land (Supplementary Figure S2). Although bias correction improved their accuracy, the combined use of dynamical downscaling and bias correction in the WRF-based experiments still produced higher accuracy, highlighting the added value of the dynamical downscaling process.

The spatial distribution of category assessments is shown in Fig. 6. Over the whole period, the POD of ERA5 and ERA5-Land is very high, with values at individual stations ranging from 0.8 to 1.0. The POD seems to be lower (higher) in the north (south) of the domain. On average, the POD is 0.90 and 0.89 for ERA5 and ERA5-Land, respectively. The POD for WRF-HCM is lower compared to the other experiments, as presented in Fig. 5. Similar to ERA5, the POD for both WRF-HCM and WRFC-HCM appears to be higher in the north and lower in the south. In all experiments, the differences between stations in each simulation are small.

The FAR of the WRF-based experiments at individual stations ranges from 0.5 to 0.7, with an average FAR of 0.60. After applying bias correction, the average FAR

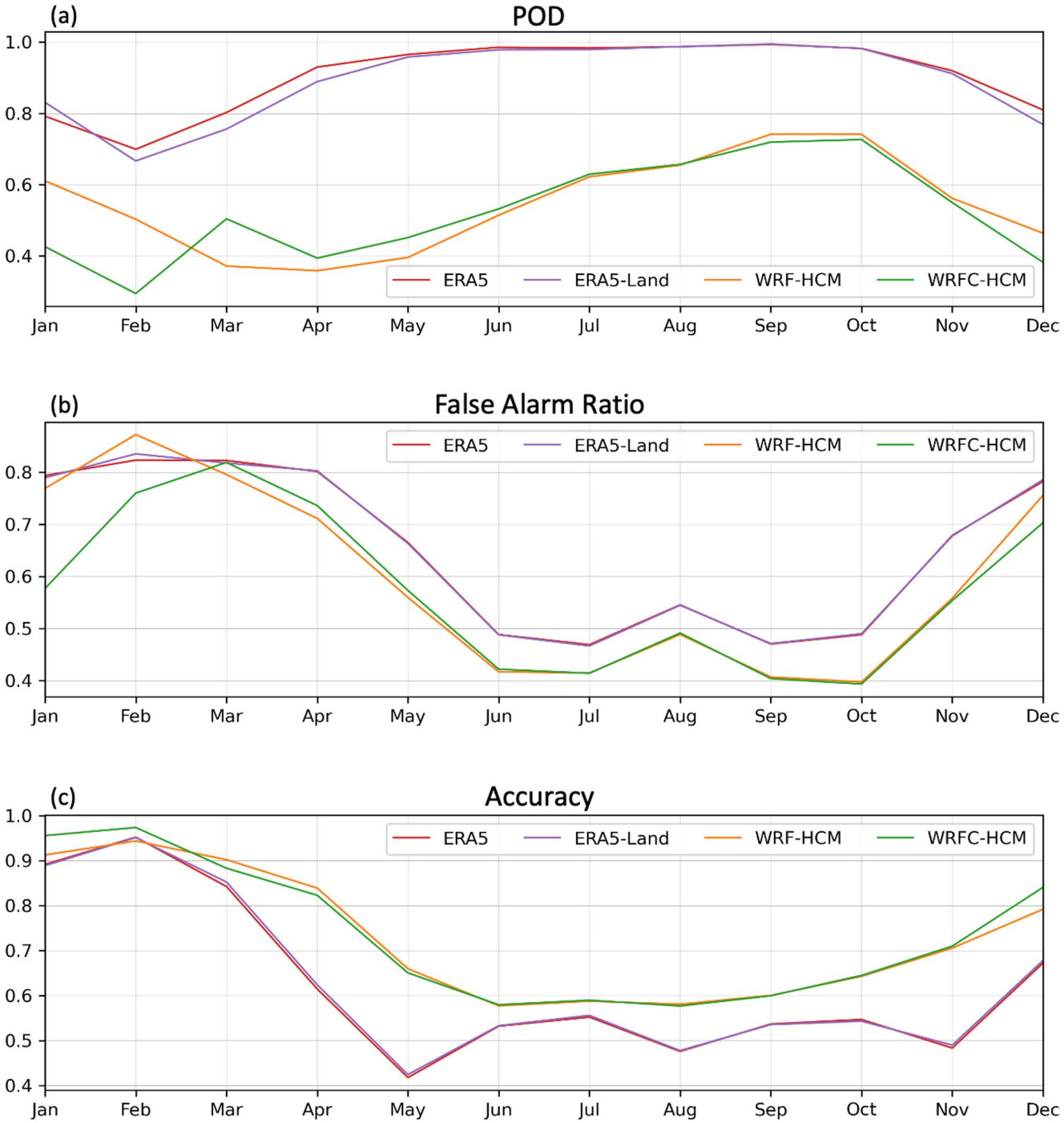

Fig. 5 Categorical assessment for daily rainfall for the different experiments: (**a**) Probability of detection, (**b**) False alarm ratio, (**c**) Accuracy

slightly improves to 0.57. These improvements are clearly shown at some stations within Ho Chi Minh City, such as stations 8 and 10. The average FAR value for ERA5 is lower, approximately 0.65. Despite the higher resolution of ERA5-Land, its FAR at individual stations remains similar to that of ERA5, ranging between 0.6 and 0.7.

While the FAR highlights false predictions, the ACC provides further insight into the overall reliability of these experiments. The ACC of WRF-HCM ranges from 0.7 to 0.8, with slightly higher values observed along the coastal areas. On average, the ACC for WRF-HCM is 0.73. Although bias correction reduces the FAR and also lowers

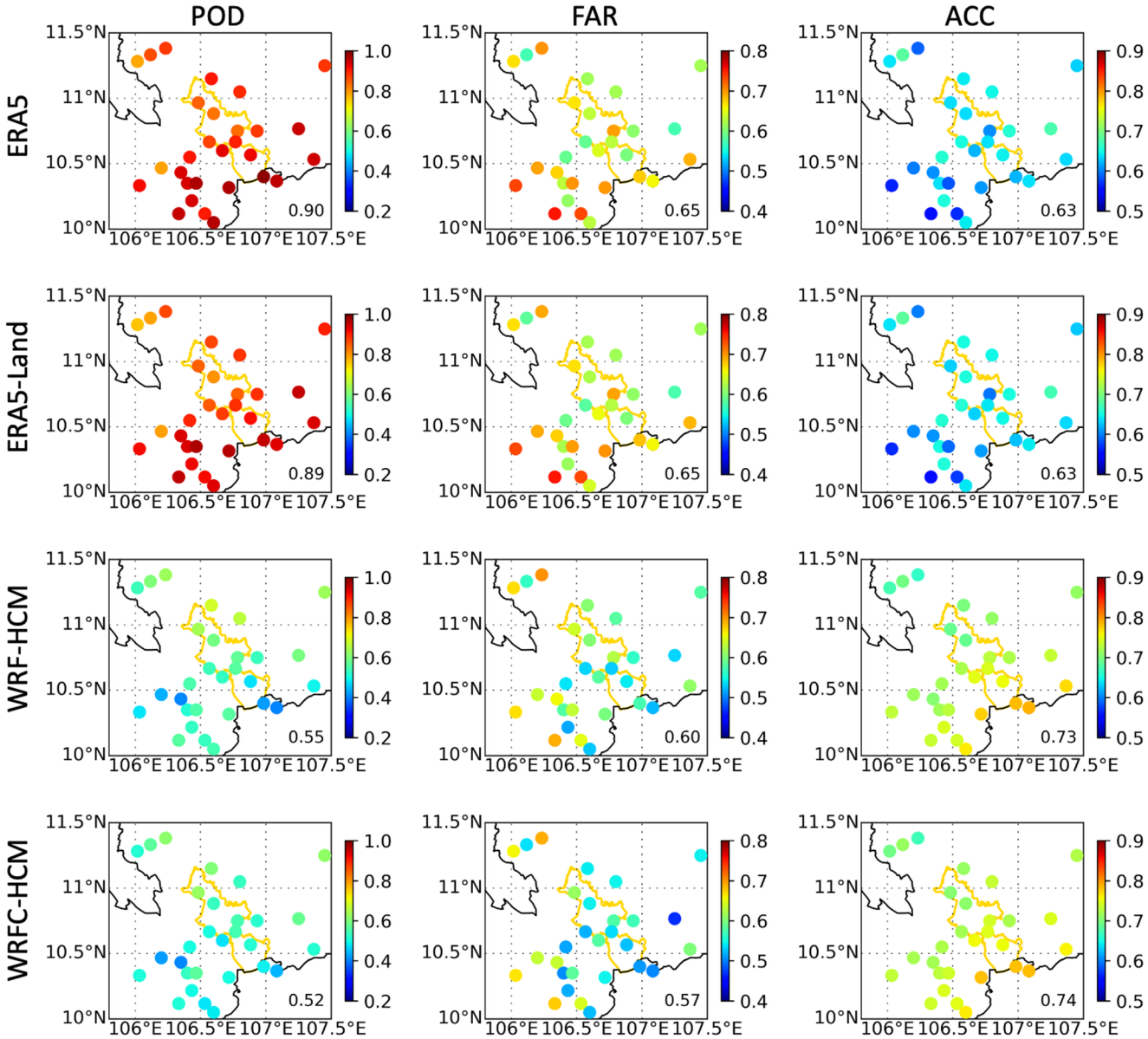

Fig. 6 POD, FAR, ACC (in column) of ERA5, ERA5-Land, WRF-HCM, and WRFC-HCM (in row), calculated using daily data, from 2010 to 2016. In each subfigure, the numbers indicate the mean values of all stations

the POD, it provides a marginal improvement in the ACC, increasing it to 0.74. In comparison, the ACC of ERA5 and ERA5-Land at individual stations is lower, ranging from 0.5 to 0.7, with an average accuracy of 0.63.

Figure 7 presents the PDF of rainfall distribution across the four seasons. During DJF, dry days (rainfall below 1 mm/day) occur approximately 95% of the time based on observations. However, all experiments underestimate the frequency of dry days. The WRF-HCM model simulates about 89% dry days, while ERA5 and ERA5-Land estimate around 80%. Bias correction significantly improves the accuracy, increasing the percentage of dry days to 94%, closely aligning with the observed value. With most days being dry, light rain events (1–5 mm/day) account for approximately 2% of days, whereas moderate (5–20 mm/day) and heavy (more than 20 mm/day) rain events are rare, each comprising about 1% of days. Among the experiments, only WRFC-HCM closely matches the observed data, whereas WRF-HCM, ERA5, and ERA5-Land tend to overestimate the number of rainy days.

In MAM, the rainfall characteristics are similar to those in DJF, with dry days occurring more than 80% of the time, while light (moderate) rainfall days account for around 5% (3%). The WRF-based experiments slightly underestimate

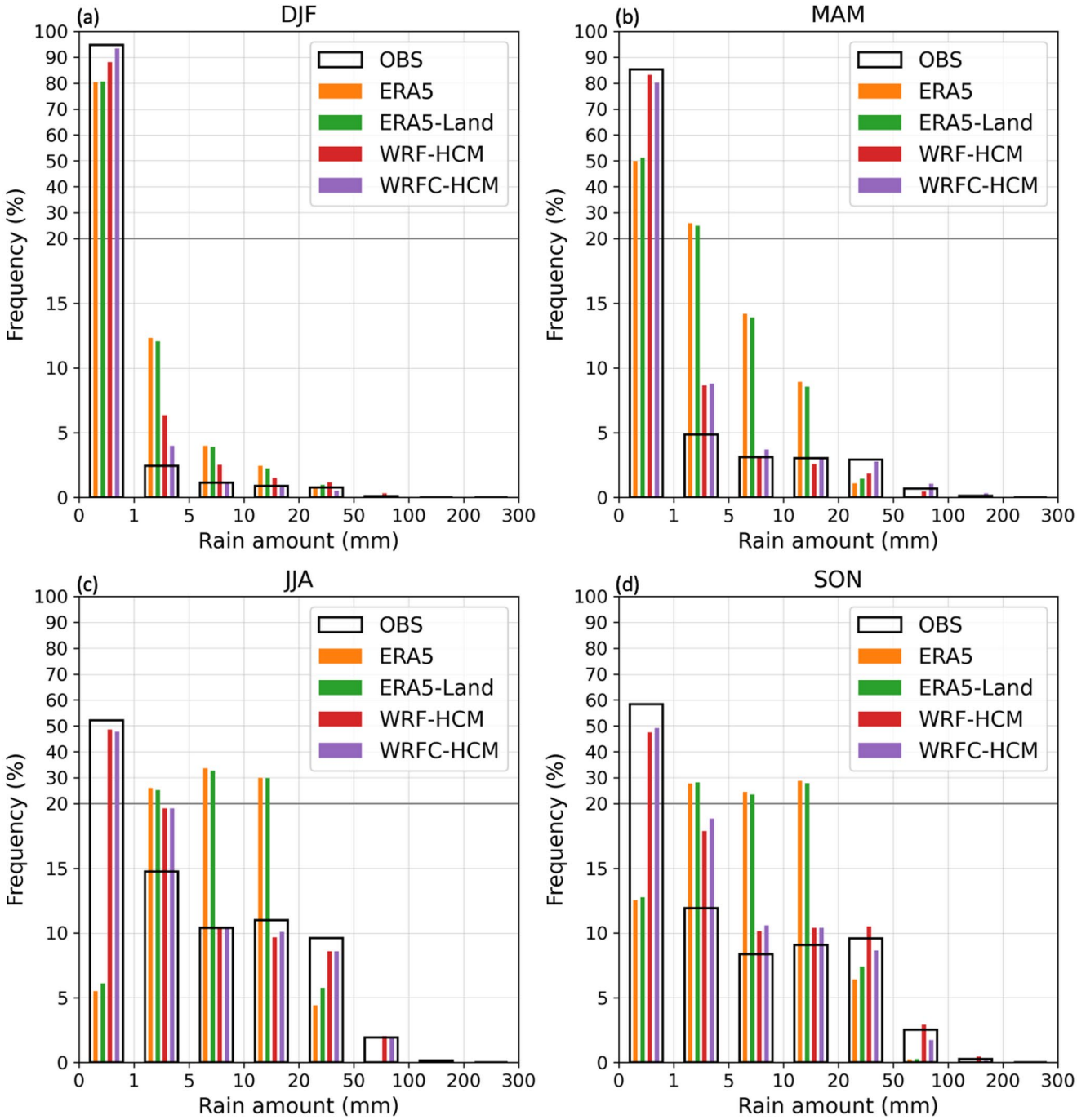

Fig. 7 Probability density function (PDF) of daily rainfall for the 4 seasons. Note that the vertical axis scale has been adjusted at a frequency level of 20% to improve representation

dry days by 5% and overestimate light rainfall days by 3%. However, they perform well in capturing moderate rainfall events. In contrast, ERA5 and ERA5-Land show significant deviations, underestimating the number of dry days by around 35% and overestimating light and moderate rainy days by 20% and 15%, respectively.

In JJA, rainfall days become more frequent, reducing the proportion of dry days to approximately 52%. However, similar to other seasons, all models underestimate the number of dry days. Specifically, ERA5 and ERA5-Land indicate only about 6% of dry days, significantly underestimating the actual proportion by 46%. This suggests that

the higher POD of ERA5 and ERA5-Land in Fig. 4a results from rain occurring almost daily. WRF-HCM and WRFC-HCM perform similarly, slightly underestimating dry days by 5%. In contrast, all experiments overestimate the number of wet days. ERA5 and ERA5-Land significantly overestimate moderate rain events at 65%, which is three times higher than observed. Meanwhile, WRF-HCM and WRFC-HCM provide consistent estimates for light rainfall days compared to observations.

In SON, the number of dry days increases to around 60%. WRF-HCM and WRFC-HCM underestimate dry days by about 10%, whereas ERA5 and ERA5-Land underestimate them by 45%. All models overestimate light rainfall days, with ERA5 and ERA5-Land showing the largest discrepancies. Moderate rainfall days are reasonably captured by WRF-HCM and WRFC-HCM but are overestimated threefold by ERA5 and ERA5-Land.

Overall, across all seasons, WRF-HCM and WRFC-HCM demonstrate better performance in modeling dry days. All experiments tend to overestimate light rainfall, with ERA5 and ERA5-Land showing the largest discrepancies. While WRF-HCM and WRFC-HCM show better accuracy in simulating medium and heavy rainfall, this remains a challenge for ERA5 and ERA5-Land.

3.3 Extremes

In addition to evaluating rainfall datasets at different time scales, it is important to assess performance during extreme events. For instance, uncertainty tend to increase as precipitation intensity rises (La Follette et al. 2021). Consequently, assessing the capability to reproduce extreme events is essential before applying a dataset to further research. In this section, we evaluate the performance of the different experiments in representing rainfall extremes using a subset of climate extreme indices recommended by the ETCCDI (Table 3).

Figure 8 illustrates the average extreme values, including those of PRCPTOT, SDII, RX1day, RX5day, CDD, and CWD, over a 7-year period (2010–2016). The observed data indicate a PRCPTOT mean of 1556.56 mm/year, with higher values (1600–1800 mm/year) in the north and lower values (1300–1400 mm/year) in the south of the city. WRF-HCM generally overestimates precipitation in the northern region and underestimates it in the south, yielding an average annual rainfall of 1656.87 mm, which exceeds the observation. Thanks to bias correction, WRFC-HCM exhibits a closer mean of 1565.82 mm/year and more consistent spatial patterns compared to the observation. In contrast, ERA5 systematically overestimates PRCPTOT across all stations, particularly in the south, and exhibits reduced spatial variability compared to the observed data. ERA5 shows a mean value of 1950.13 mm/year, approximately 20% higher than the observation. ERA5-Land demonstrates an even greater bias, with a mean of 2000.98 mm/year.

For rainfall intensity (SDII), the observed data range from 12 to 22 mm/day, with higher intensities in the northern region of the city and an average value of 15.68 mm/day. WRF-HCM and WRFC-HCM do not exhibit clear spatial patterns and slightly underestimate rainfall intensity, with mean values of 13.38 mm/day and 13.18 mm/day, respectively. In contrast, ERA5 and ERA5-Land show significant underestimation, with mean values of 8.37 mm/day and 8.79 mm/day, respectively. Despite their overestimation of PRCPTOT, the lower SDII values suggest that these datasets overestimate the number of wet days.

The RX1day and RX5day indices have observed mean values of 96.86 mm and 164 mm, respectively. WRF-HCM overestimates both indices, with mean values of 103.47 mm for RX1day and 187.12 mm for RX5day. WRFC-HCM reduces the bias for RX5day, achieving a closer mean of 173.97 mm, but slightly increases the RX1day bias to 107.99 mm, particularly along the coastal region. In contrast, ERA5 and ERA5-Land significantly underestimate these two indices. For RX1day, the mean values are 51.96 mm (ERA5) and 53.28 mm (ERA5-Land), while for RX5day, the mean values are 105.42 mm and 111.07 mm, respectively. These values correspond to only 50–65% of the observed data.

The observed CDD values range from 70 to 90 days, with an average of approximately 80 days, increasing from north to south. WRF-HCM generally underestimates CDD, with values ranging from 30 to 70 days and an average of 54 days, while maintaining the observed north-to-south spatial pattern. After bias correction, WRFC-HCM improves the estimation, increasing the average to 66 days. Both ERA5 and ERA5-Land also underestimate CDD, with averages of 53.73 days and 51.78 days, respectively.

Similarly, a validation was conducted for the bias-corrected versions of ERA5 and ERA5-Land without dynamical downscaling. The bias correction yielded notable improvements for both datasets, particularly for PRCPTOT, whose mean value after correction closely matched the observations (Supplementary Figure S3). However, improvements for the other indices were relatively modest, and the discrepancies remained substantially larger than those found in the WRF-HCM and WRFC-HCM experiments. These results highlight the added value of dynamical downscaling in enhancing rainfall representation, especially for climate extremes.

For the number of consecutive wet days (CWD), observations indicate a mean value of 8.59 days, with minimal spatial variability. WRF-HCM overestimates this value, with a mean of 14.92 days, which is reduced to 13.9 days

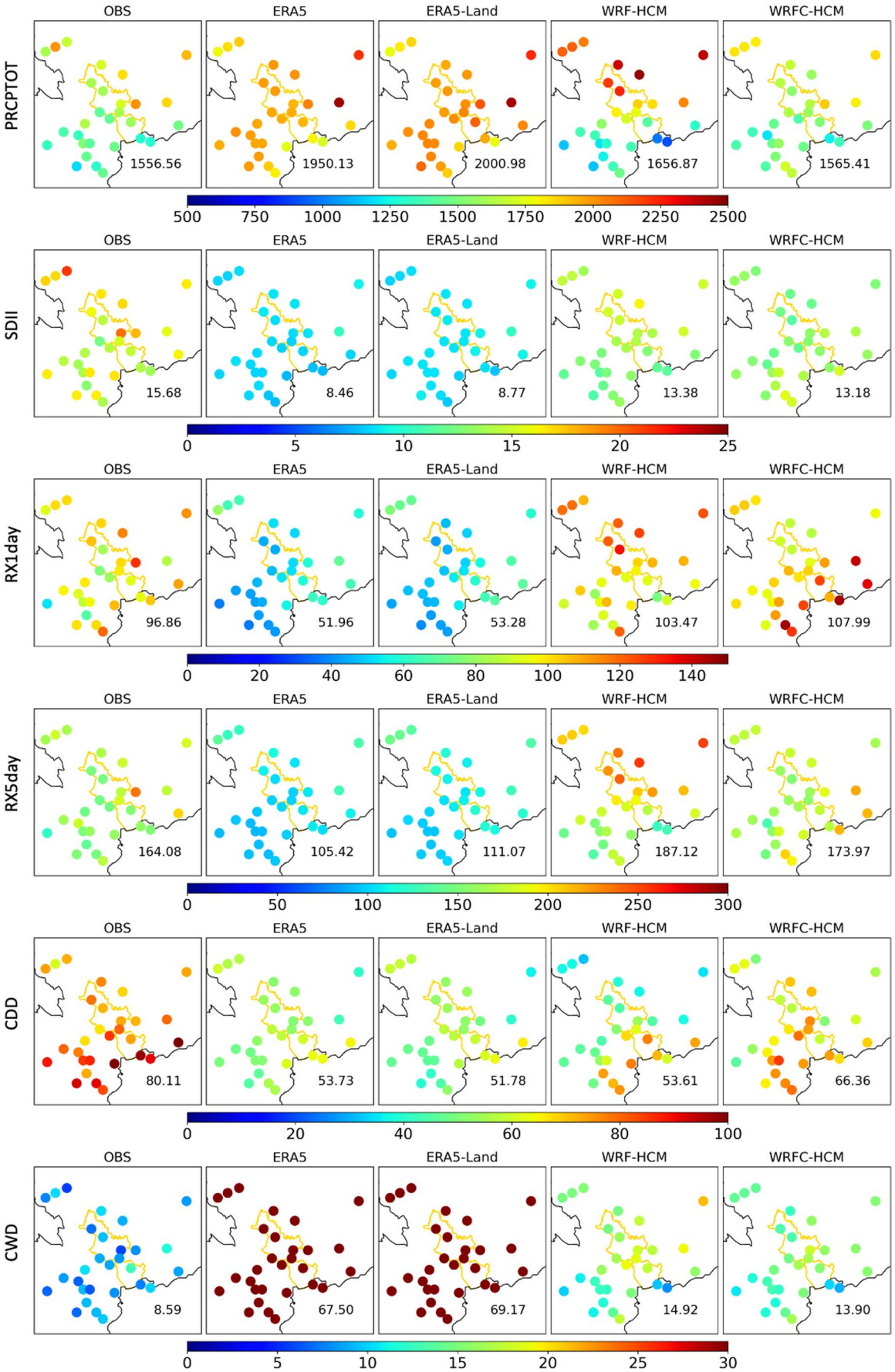
OBS
ERA5
ERA5-Land
WRF-HCM
WRFC-HCM
PRCPTOT
1556.56
1950.13
2000.98
1656.87
1565.41
500 750 1000 1250 1500 1750 2000 2250 2500
SDII
15.68
8.46
8.77
13.38
13.18
0 5 10 15 20 25
RX1day
96.86
51.96
53.28
103.47
107.99
0 20 40 60 80 100 120 140
RX5day
164.08
105.42
111.07
187.12
173.97
0 50 100 150 200 250 300
CDD
80.11
53.73
51.78
53.61
66.36
0 20 40 60 80 100
CWD
8.59
67.50
69.17
14.92
13.90
0 5 10 15 20 25 30

Fig. 8 PRCPTOT, SDII, RX1day, RX5day, CDD, CWD, averaged for 7 years from 2010 to 2016

after bias correction. As mentioned earlier, both ERA5 and ERA5-Land significantly overestimate the number of wet days, resulting in mean CWD values of 56.34 days and 68.32 days, respectively, which is around 6 to 8 times higher than the observed values.

Figure 9 presents the NMAE and NRMSE (which are the MAE and RMSE divided by standard deviation of the observation) computed temporally from 2010 to 2016. Among the selected indices, CDD shows the closest agreement with observations, indicating that the experiments capture consecutive dry days more reliably. In contrast, CWD seems challenging for all experiments and datasets. Among the experiments, WRFC-HCM consistently demonstrates the lowest errors for most indices, highlighting its ability to simulate rainfall extremes. It also demonstrates the effectiveness of bias correction in improving the accuracy and reliability of precipitation simulations compared to WRF-HCM. On the other hand, ERA5 and ERA5-Land exhibit similar performances, with relatively higher errors across all metrics, particularly for CWD.

4 Discussion

As shown in Figs. 2 and 8, WRF-HCM produces less precipitation than ERA5, which can be related to the differences in atmospheric vapor transport. Zhou et al. (2023) demonstrated that the WRF-HCM model can reduce the precipitation overestimation seen in ERA5 by limiting moisture transport over the Tibetan Plateau. To determine if this holds true for Ho Chi Minh City, we examined the integrated water vapor transport across the area for the annual average as well as for the DJF and JJA seasons (Supplementary Figure S4). In DJF, moisture transport is greater in ERA5 in the northern part of the city but comparable in the southern part, while in JJA, ERA5 shows higher moisture transport across the entire city. Nevertheless, Figs. 2 and 7 indicate that ERA5 has both higher precipitation and more wet days in both seasons, suggesting that moisture transport alone is not enough to explain the precipitation variability in this region. One hypothesis that future studies could explore is that WRF-HCM retains more atmospheric moisture due to its present physical parameterization, whereas ERA5 may convert this moisture into precipitation more efficiently, leading to the higher precipitation observed.

The precipitation bias of ERA5 has been examined in several studies, revealing varied performance across different regions and temporal scales. At the monthly scale, ERA5 has been shown to overestimate total precipitation in some areas of Africa while underestimating it in others (Steinkopf and Engelbrecht 2022). On a daily scale, Xin et al. (2022) found that ERA5, along with ERA5-Land and ERA-Interim, tends to overestimate the frequency of weak precipitation events and underestimate high-intensity rainfall. This is also the conclusion of Gomis-Cebolla et al. (2023), which is aligned with our findings. Regarding

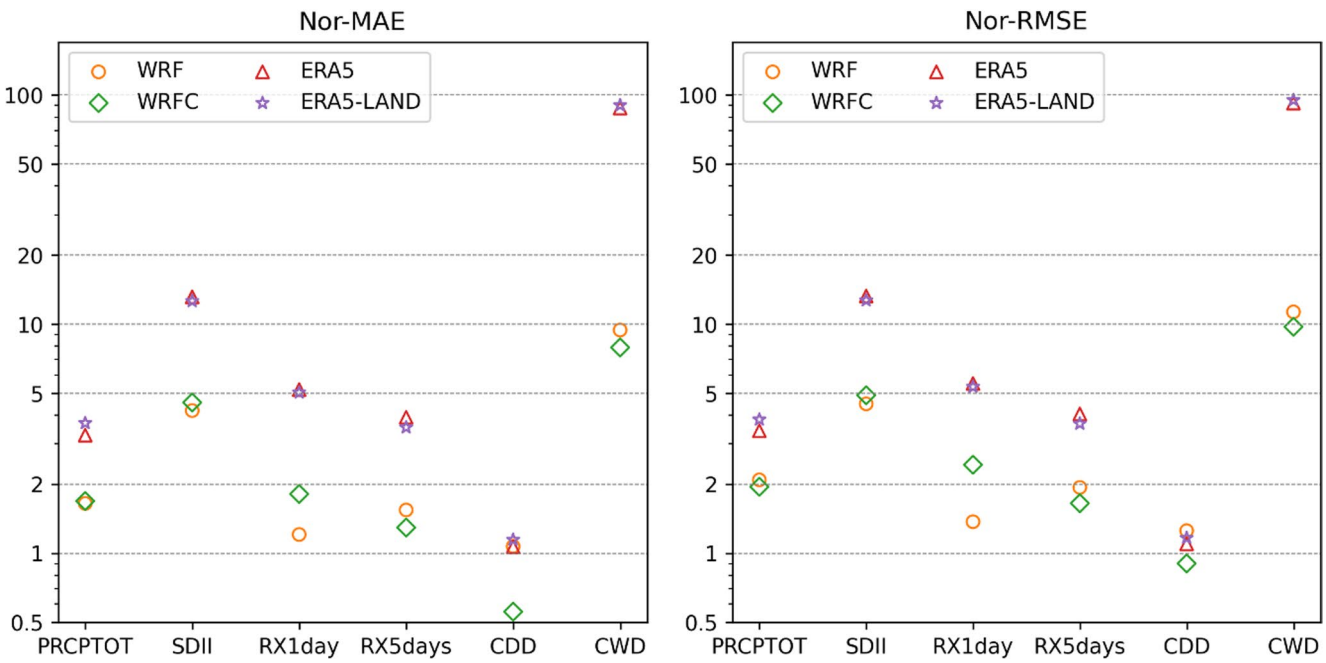

Fig. 9 Normalized Mean Absolute Error (NMAE) and Normalized Root Mean Square Error (NRMSE), computed temporally from 2010 to 2016 using station-averaged extreme indices for the different experiments (in log scale)

extreme events, Gbode et al. (2023) reported that ERA5 underestimates the frequency of heavy rainfall but overestimates the number of wet days in West Africa between 1981 and 2018, which is also consistent with our results.

Despite its higher resolution, in our study, ERA5-Land does not demonstrate significant improvement in performance compared to ERA5. This is also mentioned in other studies, e.g. Gomis-Cebolla et al. (2023). While the higher resolution of ERA5-land enables it to capture finer-scale precipitation patterns and variations, especially in regions with complex terrain (Xin et al. 2022), the lack of substantial improvement in this study may be attributed to the fact that Ho Chi Minh City is situated in a flat delta.

Considering extreme indices, our results indicate that the WRFC-HCM experiment outperforms others in both temporal and spatial aspects. This improvement is attributed to its better simulation of dry events and more accurate representation of precipitation amounts during extreme events, with the help of bias correction. Conversely, our analysis shows that ERA5 and ERA5-Land perform limitedly in simulating extreme events in HCM city. Notable differences between these datasets in representing extreme climate indices have also been reported in several studies. For instance, ERA5 has been found to overestimate CWD and underestimate the SDII (Ansari and Grossi 2022). Similar discrepancies have been observed in ERA5-LAND (Tan et al. 2023). Therefore, caution is advised when using these datasets, particularly for applications involving dry events.

After bias correction, WRFC-HCM demonstrated lower performance in March and April, possibly due to the short training period (9 years). This limited duration may prevent the quantile mapping functions derived during training from effectively capturing the variability needed to improve accuracy when applied to the validation period. Reiter et al. (2016) highlight that a shorter training period can significantly reduce the effectiveness of bias correction methods, particularly for empirical quantile mapping. To address this, future studies could use longer simulation periods to leverage the benefits of extended training durations. Accordingly, it is recommended to use longer training periods (e.g., 30 years) to construct quantile mapping functions, as demonstrated in previous studies (Tran-Anh et al. 2023; Trinh-Tuan et al. 2019).

Although WRFC-HCM demonstrates better performance at the daily scale and in capturing extreme events, there remains room for improvement. Some of the remaining biases may stem from physical processes such as convection representation, land–sea interactions, or urban heat island effects, which will be explored in subsequent studies. To further improve accuracy, upcoming research could investigate machine learning-based downscaling methods or hybrid approaches that integrate dynamical downscaling with machine learning (e.g. Tu et al. 2021), combine dynamical and statistical downscaling (Guyennon et al. 2013), or couple dynamical downscaling with atmospheric and oceanographic models to produce more integrated Earth system simulations (e.g. Li and Chen. 2022).

5 Conclusions

ERA5 is widely recognized as one of the most popular reanalysis datasets and is extensively used in various studies. However, it has two key limitations. First, its spatial resolution may not be sufficient for fine-scale applications. Second, as a global dataset, its uncertainty varies across different regions. In this study, we dynamically downscale ERA5 using the WRF model to generate a high-resolution precipitation dataset. The original ERA5 data, with a resolution of 25 km, serves as the initial and boundary conditions to produce a 2-km resolution dataset for Ho Chi Minh City. To address model bias, we apply quantile mapping, using rain gauge data for calibration and validation. The dataset from 2000 to 2009 is used for training, while the data from 2010 to 2016 is reserved for validation.

At the monthly scale, WRF-HCM dynamical downscaling shows limited improvements over the original ERA5 forcing. It performs better during the dry season (winter), but in other seasons, it results in higher errors and lower correlation. The bias correction using quantile mapping (WRFC-HCM) effectively reduces bias, but it does not improve temporal correlation. Overall, ERA5 remains the most reliable dataset for monthly precipitation estimates.

At the daily scale, WRFC-HCM demonstrates significantly higher accuracy than ERA5, particularly in capturing dry events. Seasonal probability density functions (PDFs) reveal that ERA5 strongly overestimates light rain events, whereas WRFC-HCM substantially reduces the number of false light rain detections. Additionally, ERA5 underestimates moderate and heavy rain events (exceeding 20 mm/day), while WRFC-HCM shows smaller discrepancies compared to observations. Similar to ERA5, ERA5-Land overestimates light rain occurrences and underestimates both dry and heavy rain events, making it unsuitable for short time-scale studies. The bias correction applied in WRFC-HCM is more effective during the dry season, but in the wet season, the differences between WRF-HCM and WRFC-HCM become less pronounced.

Finally, the ability to reproduce extreme climate indices was evaluated. Despite some remaining biases, WRFC-HCM performs better than other datasets in representing extreme climate events. The annual precipitation from WRFC-HCM aligns well with observations in terms of both spatial distribution and mean values. Although RX1day and

RX5days remain overestimated, their biases are smaller compared to ERA5. ERA5 and ERA5-Land demonstrate significantly higher numbers of wet days, resulting in a substantial overestimation of CWD. Conversely, these datasets underestimate the number of heavy rain events, leading to an underestimation of RX1day and RX5days. The combination of a higher total number of wet days and fewer extreme events results in an underestimation of average rainfall intensity.

Overall, the WRFC-HCM dataset demonstrates added value for high-resolution rainfall analysis in Ho Chi Minh City. Although some biases remain at the monthly scale, its improved representation of daily rainfall variability and extremes indicates potential usefulness for localized climate studies and future impact-oriented applications.

Supplementary Information The online version contains supplementary material available at https://doi.org/10.1007/s00704-025-05894-1.

Acknowledgements This work was supported by the Wellcome Trust [226052/Z/22/Z].

Author contributions Tung.N.D., Thanh.N.D. and M.C. contributed to the study conception and prepared the first draft of the manuscript. Tung.N.D processed data and performed the analysis. All authors discussed the results, read, and approved the final manuscript.

Funding This work was supported by the Wellcome Trust [226052/Z/22/Z].

Data availability The datasets generated and/or analyzed during the current study are available from the corresponding author on reasonable request.

Code availability Not applicable.

Declarations

Ethics approval This study did not involve experiments on humans or animals; therefore, ethics approval was not required.

Consent for publication Not applicable.

Consent to participate Not applicable.

Competing interests The authors declare no competing interests.

References

Almendra-Martín L, Martínez-Fernández J, Piles M, González-Zamora Á, Benito-Verdugo P, Gaona J (2022) Influence of atmospheric patterns on soil moisture dynamics in Europe. Sci Total Environ 846:157537. https://doi.org/10.1016/j.scitotenv.2022.157537

Ansari R, Grossi G (2022) Performance evaluation of raw and bias-corrected ERA5 precipitation data with respect to extreme precipitation analysis: case study in upper Jhelum Basin, South Asia. Theoret Appl Climatol 150(3):1409–1424. https://doi.org/10.1007/s00704-022-04239-6

Bastola S, Misra V (2014) Evaluation of dynamically downscaled reanalysis precipitation data for hydrological application. Hydrol Process 28(4):1989–2002. https://doi.org/10.1002/hyp.9734

Behrangi A, Khakbaz B, Jaw TC, AghaKouchak A, Hsu K, Sorooshian S (2011) Hydrologic evaluation of satellite precipitation products over a mid-size basin. J Hydrol 397(3):225–237. https://doi.org/10.1016/j.jhydrol.2010.11.043

Carvalho D, Rocha A, Gómez-Gesteira M, Silva Santos C (2014) WRF wind simulation and wind energy production estimates forced by different reanalyses: comparison with observed data for Portugal. Appl Energy 117:116–126. https://doi.org/10.1016/j.apenergy.2013.12.001

Cha D-H, Wang Y (2013) A dynamical initialization scheme for real-time forecasts of tropical cyclones using the WRF model*. Mon Weather Rev 141(3):964–986. https://doi.org/10.1175/MWR-D-12-00077.1

Chotamonsak C, Salathé EP, Kreasuwan J, Chantara S, Siriwitayakorn K (2011) Projected climate change over Southeast Asia simulated using a WRF regional climate model. Atmospheric Sci Lett 12(2):213–219. https://doi.org/10.1002/asl.313

Doan VQ, Kusaka H, Nguyen TM (2019) Roles of past, present, and future land use and anthropogenic heat release changes on urban heat island effects in Hanoi, Vietnam: numerical experiments with a regional climate model. Sustain Cities Soc 47:101479. https://doi.org/10.1016/j.scs.2019.101479

Dudhia J (1989) Numerical study of convection observed during the winter monsoon experiment using a mesoscale two-dimensional model. J Atmos Sci 46(20):3077–3107. https://doi.org/10.1175/1520-0469(1989)046%3C3077:NSOCOD%3E2.0.CO;2

Dullaart JCM, Muis S, Bloemendaal N, Aerts JCJH (2020) Advancing global storm surge modelling using the new ERA5 climate reanalysis. Clim Dyn 54(1):1007–1021. https://doi.org/10.1007/s00382-019-05044-0

El-Samra R, Bou-Zeid E, El-Fadel M (2018) To what extent does high-resolution dynamical downscaling improve the representation of climatic extremes over an orographically complex terrain? Theoret Appl Climatol 134(1):265–282. https://doi.org/10.1007/s00704-017-2273-8

Enayati M, Bozorg-Haddad O, Bazrafshan J, Hejabi S, Chu X (2021) Bias correction capabilities of quantile mapping methods for rainfall and temperature variables. J Water Clim Change 12(2):401–419. https://doi.org/10.2166/wcc.2020.261

Evans JP, Argueso D, Olson R, Di Luca A (2017) Bias-corrected regional climate projections of extreme rainfall in south-east Australia. Theoret Appl Climatol 130(3):1085–1098. https://doi.org/10.1007/s00704-016-1949-9

Feng X, Fu T-M, Cao H, Tian H, Fan Q, Chen X (2019) Neural network predictions of pollutant emissions from open burning of

crop residues: application to air quality forecasts in Southern China. Atmos Environ 204:22–31. https://doi.org/10.1016/j.atmosenv.2019.02.002

Fraga I, Cea L, Puertas J (2019) Effect of rainfall uncertainty on the performance of physically based rainfall–runoff models. Hydrol Process 33(1):160–173. https://doi.org/10.1002/hyp.13319

Gbode IE, Babalola TE, Diro GT, Intsiful JD (2023) Assessment of era5 and era-interim in reproducing mean and extreme climates over West Africa. Adv Atmos Sci 40(4):570–586. https://doi.org/10.1007/s00376-022-2161-8

Gomis-Cebolla J, Rattayova V, Salazar-Galán S, Francés F (2023) Evaluation of ERA5 and ERA5-Land reanalysis precipitation datasets over Spain (1951–2020). Atmos Res 284:106606. https://doi.org/10.1016/j.atmosres.2023.106606

GSO (2023) Statistical yearbook of Vietnam. Statistical Publishing House

Gudmundsson L, Bremnes JB, Haugen JE, Engen-Skaugen T (2012) Technical note: downscaling RCM precipitation to the station scale using statistical transformations – a comparison of methods. Hydrol Earth Syst Sci 16(9):3383–3390. https://doi.org/10.5194/hess-16-3383-2012

Gutmann ED, Rasmussen RM, Liu C, Ikeda K, Gochis DJ, Clark MP, Dudhia J, Thompson G (2012) A comparison of statistical and dynamical downscaling of winter precipitation over complex terrain. J Clim 25(1):262–281. https://doi.org/10.1175/2011JCLI4109.1

Guyennon N, Romano E, Portoghese I, Salerno F, Calmanti S, Petrangeli AB, Tartari G, Copetti D (2013) Benefits from using combined dynamical-statistical downscaling approaches – lessons from a case study in the Mediterranean region. Hydrol Earth Syst Sci 17(2):705–720. https://doi.org/10.5194/hess-17-705-2013

Hagemann S, Chen C, Haerter JO, Heinke J, Gerten D, Piani C (2011) Impact of a statistical bias correction on the projected hydrological changes obtained from three Gcms and two hydrology models. J Hydrometeorol 12(4):556–578. https://doi.org/10.1175/2011JHM1336.1

Heikkilä U, Sandvik A, Sorteberg A (2011) Dynamical downscaling of ERA-40 in complex terrain using the WRF regional climate model. Clim Dyn 37(7):1551–1564. https://doi.org/10.1007/s00382-010-0928-6

Hersbach H, Bell B, Berrisford P, Hirahara S, Horányi A, Muñoz-Sabater J, Nicolas J, Peubey C, Radu R, Schepers D, Simmons A, Soci C, Abdalla S, Abellan X, Balsamo G, Bechtold P, Biavati G, Bidlot J, Bonavita M, Thépaut J (2020) The ERA5 global reanalysis. Q J R Meteorol Soc 146(730):1999–2049. https://doi.org/10.1002/qj.3803

Hong S-Y, Lim K-SS, Lee Y-H, Ha J-C, Kim H-W, Ham S-J, Dudhia J (2010) Evaluation of the WRF double-moment 6-class microphysics scheme for precipitating convection. Adv Meteorol 2010(1):707253. https://doi.org/10.1155/2010/707253

Hong Y, Hsu K, Moradkhani H, Sorooshian S (2006) Uncertainty quantification of satellite precipitation estimation and Monte Carlo assessment of the error propagation into hydrologic response. Water Resour Res 42(8):2005WR004398. https://doi.org/10.1029/2005WR004398

Ines AVM, Hansen JW (2006) Bias correction of daily GCM rainfall for crop simulation studies. Agric for Meteorol 138(1):44–53. https://doi.org/10.1016/j.agrformet.2006.03.009

Jerez S, López-Romero JM, Turco M, Jiménez-Guerrero P, Vautard R, Montávez JP (2018) Impact of evolving greenhouse gas forcing on the warming signal in regional climate model experiments. Nat Commun 9(1):1304. https://doi.org/10.1038/s41467-018-03527-y

Kain JS (2004) The kain–fritsch convective parameterization: an update. J Appl Meteorol Climatology 43(1):170–181. https://doi.org/10.1175/1520-0450(2004)043%3C0170:TKCPAU%3E2.0.CO;2

Kumar A, Patil RS, Dikshit AK, Kumar R (2017) Application of AERMOD for short-term air quality prediction with forecasted meteorology using WRF model. Clean Technol Environ Policy 19(7):1955–1965. https://doi.org/10.1007/s10098-017-1379-0

Kusaka H, Hayami H (2006) Numerical simulation of local weather for a high photochemical oxidant event using the WRF model. JSME Int J Ser B Fluids Therm Eng 49(1):72–77. https://doi.org/10.1299/jsmeb.49.72

La Follette PT, Teuling AJ, Addor N, Clark M, Jansen K, Melsen LA (2021) Numerical daemons of hydrological models are summoned by extreme precipitation. Hydrology and Earth System Sciences 25(10):5425–5446. https://doi.org/10.5194/hess-25-5425-2021

Li S, Chen C (2022) Air-sea interaction processes during hurricane sandy: coupled WRF-FVCOM model simulations. Prog Oceanogr 206:102855. https://doi.org/10.1016/j.pocean.2022.102855

Lin Y, Colle BA (2011) A new bulk microphysical scheme that includes riming intensity and temperature-dependent ice characteristics. Mon Weather Rev 139(3):1013–1035. https://doi.org/10.1175/2010MWR3293.1

Lira-Loarca A, Berg P, Baquerizo A, Besio G (2023) On the role of wave climate Temporal variability in bias correction of gcm-rcm wave simulations. Clim Dyn 61(7–8):3541–3568. https://doi.org/10.1007/s00382-023-06756-0

Longo-Minnolo G, Vanella D, Consoli S, Pappalardo S, Ramírez-Cuesta JM (2022) Assessing the use of ERA5-Land reanalysis and spatial interpolation methods for retrieving precipitation estimates at basin scale. Atmos Res 271:106131. https://doi.org/10.1016/j.atmosres.2022.106131

Manor A, Berkovic S (2015) Bayesian inference aided analog downscaling for near-surface winds in complex terrain. Atmos Res 164–165. https://doi.org/10.1016/j.atmosres.2015.04.014

Maurer EP, Pierce DW (2014) Bias correction can modify climate model simulated precipitation changes without adverse effect on the ensemble mean. Hydrol Earth Syst Sci 18(3):915–925. https://doi.org/10.5194/hess-18-915-2014

Miao S, Chen F, LeMone MA, Tewari M, Li Q, Wang Y (2009) An observational and modeling study of characteristics of urban heat island and boundary layer structures in Beijing. J Appl Meteorol Climatol 48(3):484–501. https://doi.org/10.1175/2008JAMC1909.1

Minh PT, Tuyet BT, Thao TTT, Hang LTT (2018) Application of ensemble Kalman filter in WRF model to forecast rainfall on monsoon onset period in South Vietnam. Vietnam J Earth Sci 40(4):367–394. https://doi.org/10.15625/0866-7187/40/4/13134

Mlawer EJ, Taubman SJ, Brown PD, Iacono MJ, Clough SA (1997) Radiative transfer for inhomogeneous atmospheres: RRTM, a validated correlated-k model for the longwave. J Geophys Res Atmos 102(D14):16663–16682. https://doi.org/10.1029/97JD00237

Muñoz-Sabater J, Dutra E, Agustí-Panareda A, Albergel C, Arduini G, Balsamo G, Boussetta S, Choulga M, Harrigan S, Hersbach H, Martens B, Miralles DG, Piles M, Rodríguez-Fernández NJ, Zsoter E, Buontempo C, Thépaut J-N (2021) ERA5-land: a state-of-the-art global reanalysis dataset for land applications. Earth Syst Sci Data 13(9):4349–4383. https://doi.org/10.5194/essd-13-4349-2021

Ngo-Duc T, Nguyen-Duy T, Desmet Q, Trinh-Tuan L, Ramu L, Cruz F, Dado JM, Chung JX, Phan-Van T, Pham-Thanh H, Truong-Ba K, Tangang FT, Juneng L, Santisirisomboon J, Srisawadwong R, Permana D, Linarka UA, Gunawan D (2024) Performance ranking of multiple CORDEX-SEA sensitivity experiments: towards an optimum choice of physical schemes for RegCM over

Southeast Asia. Clim Dyn 62:8659–8673. https://doi.org/10.1007/s00382-024-07353-5

Nguyen-Thanh H, Ngo-Duc T, Herrmann M (2023) The distinct impacts of the two types of ENSO on rainfall variability over Southeast Asia. Clim Dyn 61(5):2155–2172. https://doi.org/10.1007/s00382-023-06673-2

Reiter P, Gutjahr O, Schefczyk L, Heinemann G, Casper M (2018) Does applying quantile mapping to subsamples improve the bias correction of daily precipitation? Int J Climatol 38(4):1623–1633. https://doi.org/10.1002/joc.5283

Reiter P, Gutjahr O, Schefczyk L, Heinemann G, Casper M (2016) Bias correction of ENSEMBLES precipitation data with focus on the effect of the length of the calibration period. Meteorol Z. https://doi.org/10.1127/metz/2015/0714

Sangelantoni L, Russo A, Gennaretti F (2019) Impact of bias correction and downscaling through quantile mapping on simulated climate change signal: a case study over central Italy. Theoret Appl Climatol 135(1):725–740. https://doi.org/10.1007/s00704-018-2406-8

Seenu PZ, Jayakumar K (2020) Optimization of bias correction methods for Rcm precipitation data and their effects on extremes. Numer Optim Eng Sci 83–91. https://doi.org/10.1007/978-981-15-3215-3_9

Skamarock WC, Klemp JB, Dudhia J, Gill DO, Liu Z, Berner J, Wang W, Powers JG, Duda MG, Barker DM, Huang X-Y 2019: A Description of the Advanced Research WRF Version 4. NCAR Tech. Note NCAR/TN-556+STR, 145 pp. https://doi.org/10.5065/1dfh-6p97

So D, Shin D (2018) Classification of precipitating clouds using satellite infrared observations and its implications for rainfall estimation. Q J R Meteorol Soc 144(S1):133–144. https://doi.org/10.1002/qj.3288

Srivastava PK, Islam T, Gupta M, Petropoulos G, Dai Q (2015) Wrf dynamical downscaling and bias correction schemes for Ncep estimated hydro-meteorological variables. Water Resour Manage 29(7):2267–2284. https://doi.org/10.1007/s11269-015-0940-z

Steinkopf J, Engelbrecht F (2022) Verification of ERA5 and ERA-Interim precipitation over Africa at intra-annual and interannual timescales. Atmos Res 280:106427. https://doi.org/10.1016/j.atmosres.2022.106427

Tabari H (2020) Climate change impact on flood and extreme precipitation increases with water availability. Sci Rep 10(1):13768. https://doi.org/10.1038/s41598-020-70816-2

Tamaki Y, Inatsu M, Nguyen-Le D, Yamada TJ (2018) Heavy rainfall duration bias in dynamical downscaling and its related synoptic patterns in summertime Asian monsoon. J Appl Meteorol Climatol 57(7):1477–1496. https://doi.org/10.1175/JAMC-D-17-0116.1

Tan ML, Armanuos AM, Ahmadianfar I, Demir V, Heddam S, Al-Areeq AM, Abba SI, Halder B, Cagan Kilinc H, Yaseen ZM (2023) Evaluation of NASA POWER and ERA5-Land for estimating tropical precipitation and temperature extremes. J Hydrol 624:129940. https://doi.org/10.1016/j.jhydrol.2023.129940

Thanh Tu T, Nitivattananon V (2011) Adaptation to flood risks in Ho Chi Minh city, Vietnam. Int J Clim Change Strateg Manag 3(1):61–73. https://doi.org/10.1108/17568691111107943

Themeßl M, Gobiet A, Leuprecht A (2011) Empirical-statistical downscaling and error correction of daily precipitation from regional climate models. Int J Climatol 31(10):1530–1544. https://doi.org/10.1002/joc.2168

Tien DD, Ngo-Duc T, Mai HT, Kieu C (2013) A study of the connection between tropical cyclone track and intensity errors in the WRF model. Meteorol Atmos Phys 122(1):55–64. https://doi.org/10.1007/s00703-013-0278-0

Tran-Anh Q, Ngo-Duc T, Espagne E, Trinh-Tuan L (2023) A 10-km CMIP6 downscaled dataset of temperature and precipitation for historical and future Vietnam climate. Sci Data 10(1):257. https://doi.org/10.1038/s41597-023-02159-2

Tran Anh Q, Taniguchi K (2018) Coupling dynamical and statistical downscaling for high-resolution rainfall forecasting: case study of the red river Delta, Vietnam. Prog Earth Planet Sci 5(1):28. https://doi.org/10.1186/s40645-018-0185-6

Trinh T, Do N, Nguyen VT, Carr K (2021) Modeling high-resolution precipitation by coupling a regional climate model with a machine learning model: an application to Sai Gon-Dong Nai rivers basin in Vietnam. Clim Dyn 57(9):2713–2735. https://doi.org/10.1007/s00382-021-05833-6

Trinh-Tuan L, Matsumoto J, Tangang FT, Juneng L, Cruz F, Narisma G, Santisirisomboon J, Phan-Van T, Gunawan D, Aldrian E, Ngo-Duc T (2019) Application of quantile mapping bias correction for mid-future precipitation projections over Vietnam. Sola 15:1–6. https://doi.org/10.2151/sola.2019-001

Tu T, Ishida K, Ercan A, Kiyama M, Amagasaki M, Zhao T (2021) Hybrid precipitation downscaling over coastal watersheds in Japan using WRF and CNN. J Hydrol Reg Stud 37:100921. https://doi.org/10.1016/j.ejrh.2021.100921

Ukkola AM, De Kauwe MG, Roderick ML, Abramowitz G, Pitman AJ (2020) Robust future changes in meteorological drought in CMIP6 projections despite uncertainty in precipitation. Geophys Res Lett 47(11):e2020GL087820. https://doi.org/10.1029/2020GL087820

Vu T-T, Thy PTM, Nguyen LĐ (2018) Multiscale remote sensing of urbanization in Ho Chi Minh city, Vietnam—a focused study of the South. Appl Geogr 92:168–181. https://doi.org/10.1016/j.apgeog.2017.12.026

Winterbottom HR, Uhlhorn EW, Chassignet EP (2012) A design and an application of a regional coupled atmosphere-ocean model for tropical cyclone prediction. J Adv Model Earth Syst 4(4):2012MS000172. https://doi.org/10.1029/2012MS000172

Xin Y, Yang Y, Chen X, Yue X, Liu Y, Yin C (2022) Evaluation of Imerg and era5 precipitation products over the Mongolian plateau. Sci Rep 12(1):21776. https://doi.org/10.1038/s41598-022-26047-8

Zhang X, Xiong Z, Zheng J, Ge Q (2018) High-resolution precipitation data derived from dynamical downscaling using the WRF model for the Heihe river basin, Northwest China. Theoret Appl Climatol 131(3):1249–1259. https://doi.org/10.1007/s00704-017-2052-6

Zhuo L, Dai Q, Han D, Chen N, Zhao B (2019) Assessment of simulated soil moisture from WRF Noah, Noah-MP, and CLM land surface schemes for landslide hazard application. Hydrol Earth Syst Sci 23(10):4199–4218. https://doi.org/10.5194/hess-23-4199-2019

Zhou P, Shao M, Ma M, Ou T, Tang J (2023) WRF gray-zone dynamical downscaling over the Tibetan plateau during 1999–2019: model performance and added value. Clim Dyn 61(3):1371–1390. https://doi.org/10.1007/s00382-022-06631-4